Pis'ma ZhETF (Sov.) 3 (1977) 1257.
4 KHARCHENKO I.F., FAINBERG Ya.B., KORNILOV E.A. et al. Proc. of IV Intern. Conf. on Ioniz. Phenomena in Gases, Uppsala, 17-21 August (1959), 2 (1960), p. IIIB-671.
5 FAINBERG Ya.B., Atomnaya En (Sov.) 11, N°10 (1961) 313.
6 VEDENOV A.A., VELIKHOV E.P., SAGDEEV R.Z., Uspekhi Fiz. Nauk (Sov.) 73, N°4 (1961) 701.
7 GOTT Yu.V., Vzaimodejstvie chastits s veshchestvom v plazmennykh issledovaniyakh (Particle-substance interactions in plasma studies). Moscow, Atomizdat (1978).
8 KORNILOV E.A., KOVPIK O.F., FAINBERG Ya.B., KRAVCHENKO G.F., Fizika plasmy i problemy upravlyaemogo termoyadernogo sinteza (Plasma physics and controlled fusion research), Kiev, "Naukova Dumka" publ., N°4 (1965) 145.
9 IVANOV A.A., KRASHENINNIKOV S.G., SOBOLEVA T.K., YUSHMATOV P.N., Fiz.Plasmy (Sov.) 1 (1975) 753.
10 PISTUNOVICH V.G., PLATONOV V.V., RYUTOV V.D., FILIMONOV V.A., Fiz.Plasmy 2 (1976) 751.

Reprint from
Proceedings of the
3rd International Topical Conference on
High Power Electron and Ion Beam
Research and Technology
Vol. I

Novosibirsk, 1979

INTERACTION OF REB WITH A PLASMA CLUSTER

P.Šunka, K.Jungwirth, I.Kováč, J.Stöckel, V.Piffl, J.Ullschmied
Institute of Plasma Physics
Prague, CSSR

1. INTRODUCTION

Interaction of a high-power relativistic electron beam with a plasma cluster is investigated following the two main directions:

a) Beam transport through a magnetized plasma column and plasma heating by the propagating relativistic electron beam (REB).
b) Reflexing electron beam phenomena, plasma heating, and ion acceleration in system with a virtual cathode.

Propagation of REB through a plasma is limited by the two-stream instability and return current dissipation. As the contribution of collective processes to the beam energy loss decreases and collisional loss increases at higher plasma densities, an optimum density (10^{21} - 10^{22} m^{-3}) should exist permitting an almost lossless beam transport. Efficient plasma heating occurring at lower plasma densities is completely determined by collisionless processes /1-3/.

The virtual cathode is created spontaneously at the plasma-vacuum boundary by the uncompensated space charge of the beam and it reflects most of the beam electrons if I_b substantially exceeds the vacuum critical current I_v. In a strong external magnetic field the electrons confined radially and trapped axially between the real and the virtual cathodes form an oscillating relativistic electron beam (OREB). The energy stored in OREB electrons could be transferred partly to a plasma enhancing especially heating of relatively short plasma, partly to energetic ions collectively accelerated from the plasma boundary, as well as to an intense microwave radiation /4,5/.

2. EXPERIMENTAL ARRANGEMENT

Measurements have been performed on the improved REBEX machine /6/ schematically shown in Fig.1. The beam (500 keV, 20-30 kA, 70ns, 28 mm in diameter) is injected into a conducting vacuum chamber (D = 150 mm, L = 2,1 m) containing neutral gas or a hydrogen plasma

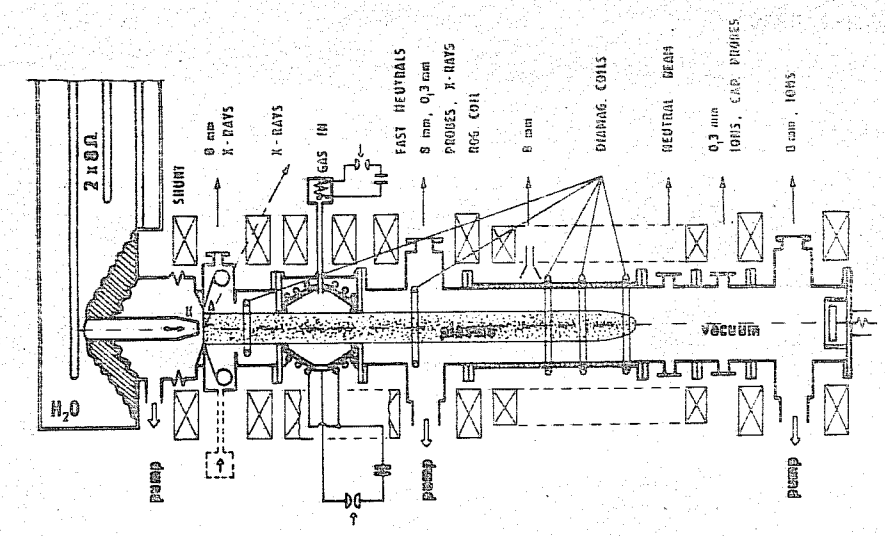

Fig.1 Schematic of the REBEX device and location of some diagnostics

from a double conical gun which is located near the beam entrance. The gun-generated plasma (70 mm in diameter) expands along the external magnetic field (mirror ratio 1,5; B_{max}= 0,7 T) with a velocity of 2-4.$10^4 ms^{-1}$. Time dependence of plasma density measured at cross-sections z_1 = 50 cm and z_2= 200 cm (8 mm, 0,3 mm interferometers and neutral beam probing) is shown in Fig. 2 (the gun fires at t_d = 0). The maximum plasma density of a short cluster (60 cm) is about $10^{21} m^{-3}$ and it decreases to $10^{20} m^{-3}$ for the full-length plasma. By varying the time delay t_d between firing the gun and the beam, both propagating (REB) and oscillating (OREB) beam regimes can be adjusted.

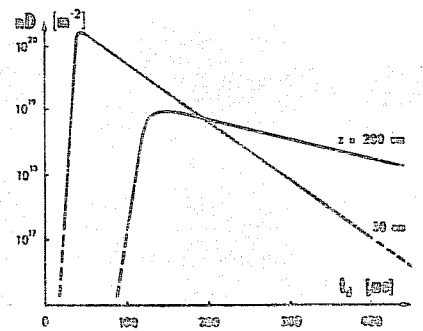

Fig.2 Time variations of plasma density at two cross-sections of the REBEX chamber

3. BEAM TRANSPORT AND PLASMA HEATING

Transport of the beam and plasma heating are investigated for various time delays t_d between the plasma and beam injections. Efficiency of the beam current transport I_c/I_D is plotted in Fig.3. (I_c, I_D are the collector and diode currents respectively.) It is maximum (85%) at t_d=150 μs when the plasma is almost homogeneous along the system. At t_d>150μs the transported current decreases gradually with the decreasing plasma density. For t_d < 80 μs only critical vacuum current (I_v = 1,5 kA) flows to the collector indicating that regimes with a virtual cathode are established.

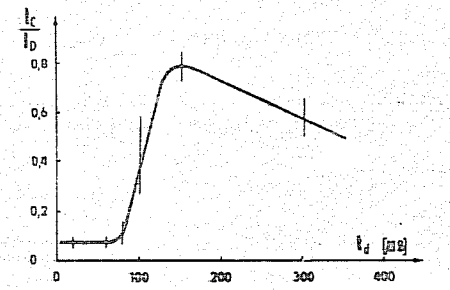

Fig.3 Transported beam current I_c/I_D versus the time delay t_d between the plasma and beam injections

To evaluate the plasma energy content (heating efficiency) the plasma diamagnetism ($nT_\perp S$) is measured by a set of single-turn self-integrating coils located at distances z = 10, 50, 100, 120 and 140 cm from the anode. The maximum diamagnetism is observed at the end of the beam injection (t=70 ns). By using the diamagnetic data the total transverse energy Q stored in a plasma can be determined from the reconstructed longitudinal profiles of $nT_\perp S$. These profiles are depicted in Fig.4 for several characteristic values of t_d. The total energy Q reaches its maximum Q=150 J for t_d = 40 μs and it falls

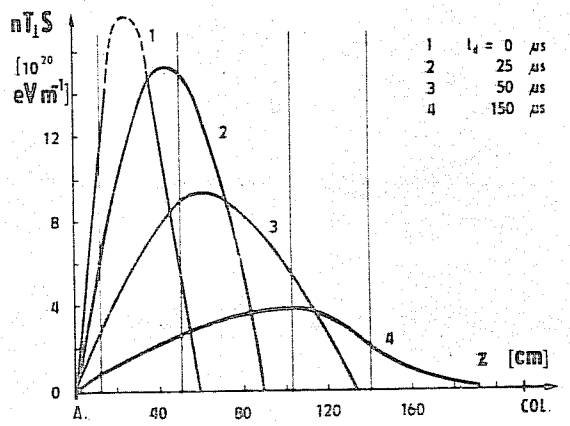

Fig.4 Longitudinal profiles of the plasma diamagnetism for several delays t_d

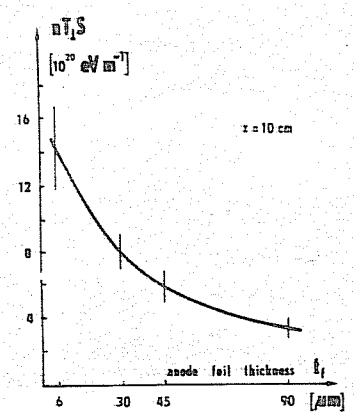

Fig.5 Dependence of plasma diamagnetism on the anode foil thickness

to Q = 45 J in the optimum beam transport regime (t_d = 150 μs). Comparing these values with the total energy of the injected beam (Q_b = 450 J) the heating efficiencies of 30 % and 10 % are obtained respectively. Effect of the anode foil thickness on the heating efficiency is illustrated in Fig.5. Apparently, the stronger beam scattering on thicker foils results in weakening the interaction.

In most regimes the diamagnetic signal displays regular damped oscillations with a frequency corresponding to magnetosonic bouncing of the plasma column. The hot plasma core tends to expand radially to establish equilibrium pressure balance between the particles and magnetic field. To get more information on these processes, the local, time-resolved magnetic probe measurements have been done for several delays t_d. Evolution of the radial profile of the magnetic field $\Delta B(r,t)$ is shown in Fig.6 for t_d = 50 μs. Position of the turning point from dia-to paramagnetism $\Delta B(r_0,t) = 0$ (indicated by the dashed line) determines the instantaneous radius of a hot plasma core. Starting at the beam radius it oscillates in a similar manner as the diamagnetic signal thereafter. As the diffusion time of the magnetic field through the surrounding cold plasma is some 100 ns (cf.Fig.6), the radial profile $\Delta B(r,t)$ has to be accounted for proper interpretation of the diamagnetic loop measurements. By decreasing plasma density (increasing t_d) the

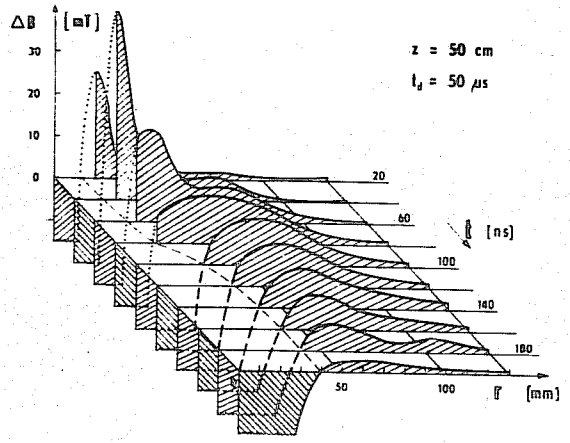

Fig.6 Time evolution of the radial profile of magnetic field $B(r,t)$, t_d=50 μs

diffusion time becomes shorter than the pulse duration and the oscillations of the diamagnetic signals are strongly damped. From the monotonous long-time behaviour of the diamagnetic signals the life-time of the heated plasma may be deduced (< 1 μs). In the case of optimum plasma heating the diamagnetic field almost compensates the external field B_o on the axis. The diameter of the hot plasma core exceeds roughly twice that of the beam.

Using the measured data on hot plasma core, also the mean plasma energy densities nT corresponding to the optimum heating regimes by REB and OREB can be compared. Following Fig.7, the 2-3 times higher total energy transfer in the OREB regime results in the increase in the plasma energy density nT by an order of magnitude.

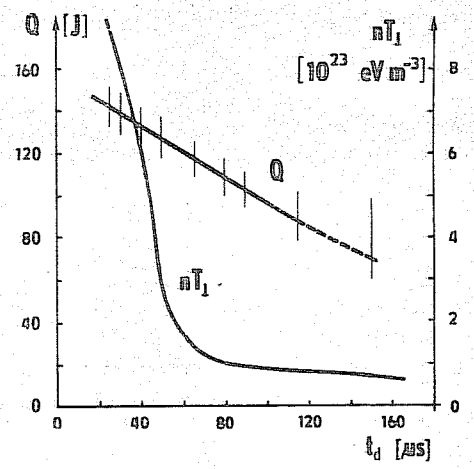

Fig.7 Total energy Q stored in plasma and mean plasma energy density nT versus the time delay t_d

Additional measurements were performed to estimate the distribution of energy between electron and ion plasma components. Ions leaving the plasma along magnetic axis are analyzed. The measured ion drift and thermal energies are both close to 100 eV. Temperature of the bulk of plasma electrons should be comparable with this value, as the ions get their energy mainly due to the expansion of the hot-electron plasma body. Soft X-ray spectra are measured by a multichannel analyzer with the detection threshold of about 3 keV which proved to be too high to determine the electron temperature of the plasma body. Nevertheless, a hot tail living several tens of μs is observed in OREB regimes and bursts of energetic photons (E ≥ 100 keV) are detected even for more than 200 μs.

4. REFLEXING BEAM PHENOMENA AND ION ACCELERATION

Higher heating rates in OREB regimes (increasing for shorter and denser plasma columns) are associated with the existence of the virtual cathode. When destroying the virtual cathode by placing the collector closely enough to the plasma boundary, the heating efficiency falls at least by an order of magnitude as demonstrated in Fig. 8. In REBEX machine the location and effective length of the virtual cathode, where most of beam electrons are reflected, are determined from the dependence of the beam current on the position of a movable collector. The effective length is minimum (25mm) in the case of the foil-terminated plasma, it is somewhat longer for the shortest plasma clusters and it extends to 300 mm for a diffuse plasma. Obviously, the potential distribution of the virtual cathode is roughly one-dimensional only in the two former cases.

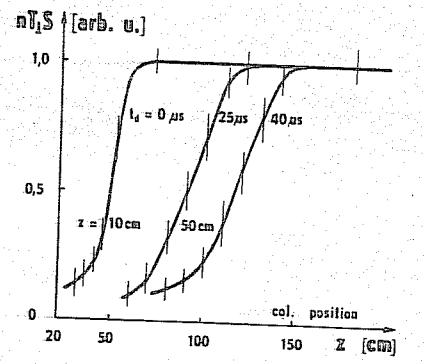

Fig.8 Dependence of plasma diamagnetism on the position of a movable collector

Further, the collector and X-ray measurements proved the existence of an oscillating electron cloud (OREB)/4,5/. Even with the thinnest anode foil (6 μm Al) the beam electrons complete not more than 4 cycles between the virtual cathode and the real one. Excessive losses due to the scattering in foils and to the intense beam-plasma interaction are responsible for the relatively low accumulation rates.

Complementary information on the dynamics of the virtual cathode is carried by the collectively accelerated ions /7/. Therefore, the total number, energy spectrum, time and place of origin of high-energy ions ($E_i > 60$ keV) are determined in various arrangements with foil diodes (beam injection into vacuum, puff of neutral H_2 and D_2, and short plasmoid) or a dielectric-anode foilless diode. Faraday cups and time-of-flight methods are used for ion energy analysis. The total number and the maximum energy of ions are determined also by nuclear target techniques. The results of measurements are summarized in the Table 1, where the total number of particles, maximum energy of ions and particle acceleration efficiency are listed for various types of injection. Just the maximum values for each regime are presented. When reducing the foil thickness, the total number of accelerated ions increases but the high-energy part of the ion spectrum remains unchanged i.e. it is not influenced by the increasing beam accumulation.

ACCELERATED IONS	BEAM INJECTION TYPE						
	NEUTRAL GAS		PLASMA		FOIL ONLY		DIELECTRIC HOLLOW ANODE
	B≠0	B=0	L=0,3m	L=1,6m	t=30μm	t=6μm	
TOTAL NUMBER $E_i \geq 60$ keV	7.10^{13}	$1,5.10^{12}$	2.10^{13}	7.10^{12}	1.10^{12}	7.10^{13}	$1,7.10^{13}$
$E_i \geq 350$ keV	2.10^{13}	$1,5.10^{12}$	5.10^{12}	0	0		2.10^{12}
MAX. ENERGY E_{imax}/E_0	2-2,4	3-3,5	0,5-1	0,2-0,5	0,5-0,7		3 - 4
MEAN ENERGY $\langle E_i \rangle / E_0$	1	2	1	1	1	1	?
EFFICIENCY $\eta_p = N_i/N_0$	2,3%	0,04%	0,7%	0,2%	0,03%	2,3%	0,6 %

Table 1. Longitudinally accelerated ions for various beam injection types

In the only regime - that with the diffuse plasma boundary - transversally accelerated ions are ejected from the virtual cathode region of the effective length of 20-30 cm. Their maximum energy ($E_i \geq 400$ keV) is comparable with that of the injected beam. The burst-like appearence of these ions (of duration of about 10 ns) provide direct evidence of the non-stationary nature of the virtual cathode and of its complicated spatial structure /2/.

In addition to the described measurements and to the extensive theoretical work we started also numerical simulations to complement the experimental and theoretical results (qualitative estimates) concerning various processes in OREB systems.

5. THE $1\frac{1}{2}$-D MODEL OF A REFLEX TRIODE COUPLED TO EXTERNAL CIRCUIT

Complex simulation model was deviced to investigate dynamics of various reflexing beam phenomena, ion beam generation or ion acceleration as well as matching the diode to power generator /8,9/.

Central module - the PIC simulation code OREBIA operates at an arbitrarily shaped diode voltage pulse $U_b(t)$ and covers both the high-voltage diode and intermediate (e.g. plasma column), virtual cathode and drift regions. In Figs. 9-11 reflex triode performance in two regimes is illustrated, the second run accounted also for an ion cloud within the diode and for generation of a drifting ion beam at $T > 50$. (T is scaled to the electron time of flight through the diode.) Fast undamped changes of the diode current I_e and of the potential distribution indicate that the oscillating nature of such systems, revealed in the earlier 1D simulation of a steady-beam injection into vacuum /3/, is only slightly affected by the accumulation of beam electrons. (The foil permits some 10 crossings per a $\gamma = 2$-$2{,}5$ electron) Such changes of I_e can hardly be followed by the external circuit. Moreover, I_e can increase by more than an order of magnitude (Fig10) without any sign of saturation, whereas in the pulse-forming line the current cannot exceed twice the matched load value. Ion extraction limited only by the space-charge effects and overcritical mean number of the anode-foil crossings are the dominant causes for transition from "saturated" (Fig.9) to "unsaturated" (Fig.10) regimes. Only in the former case the OREBIA code operated at fixed U_b yields after time averaging an(zero order) information on a final quasi-steady state.

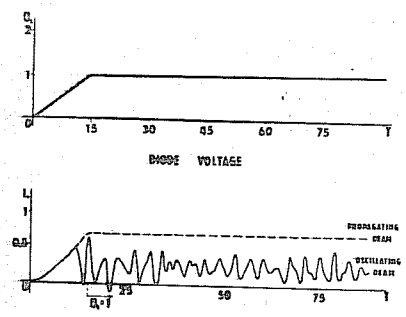

Fig.9 Diode current without ions

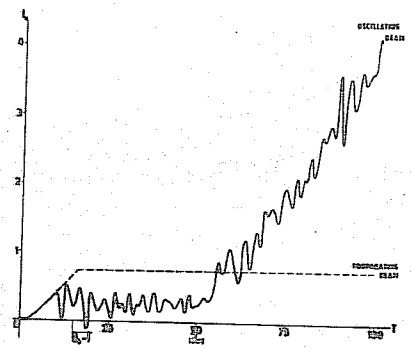

Fig.10 Diode current with ions

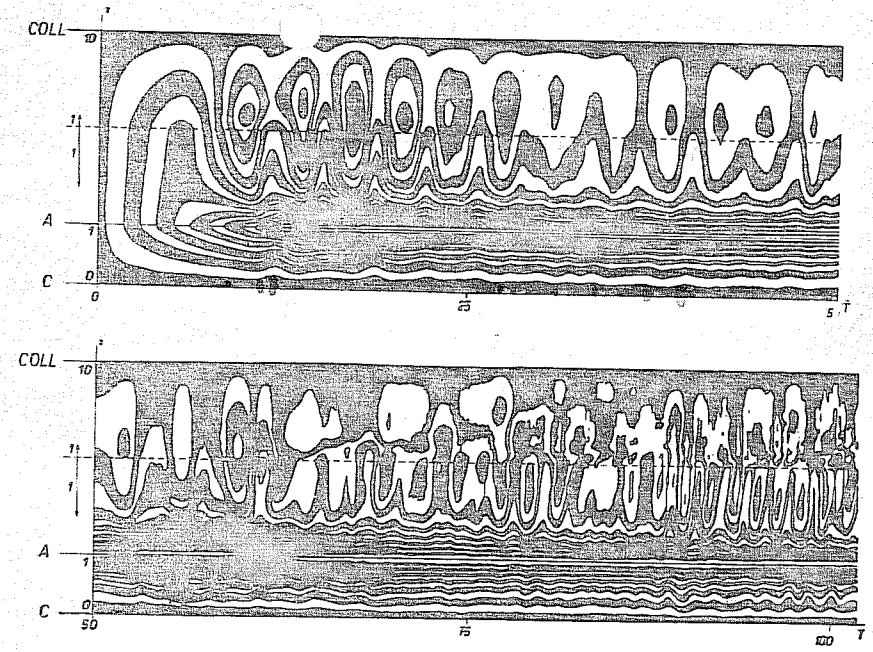

Fig.11 Time evolution of potential distribution ($\gamma = 2$, $m_i/m_e = 100$)

Generally, $U_b(t)$ has to be determined selfconsistently, as in the OREB regimes the real diode voltage exhibits fast oscillations and its mean value can be reduced during the main pulse to such an extent that any quasi-steady approach with fixed $U_b(t)$ is unadequate. For these reasons we set ut two versions of rather sophisticated code REX simulating performance of the external circuit coupled with a diode model (e.g. OREBIA). The intrinsic numerical stability of the REX scheme was achieved by accounting also for the capacity of the diode structure. Test runs proved e.g. that the results of computer simulation of a simple diode (without ions) fit very well (dashed lines in Figs. 9,10) with that obtained by a direct numerical solution based on the modified Child-Langmuir law. At present we operate the complex OREBIA-REX with the aim to match optimally the circuit and diode parameters and to find the optimum conditions for both ion beam generation and electron accumulation.

6. CONCLUSIONS

The REBEX machine permitted us to compare the efficiency of plasma heating in propagating (REB) and oscillating (OREB) beam regimes. The propagating beam energy loss decreases with increasing the plasma density. The best transport (85%) was achieved at the highest plasma density ($10^{20} m^{-3}$). Plasma heating is completely due to the two-stream instability in this regime.

In the OREB regime the plasma energy content is 2-3 times higher, although the plasma column is shorter and its density ($10^{21} m^{-3}$) is more inhomogeneous. The corresponding plasma energy density nE exceeds then by an order of magnitude that of a plasma heated optimally by a propagating REB.

Simultaneously, ions are collectively accelerated from the plasma boundary. This process is most efficient in systems with an effectively one-dimensional virtual cathode.

First results were obtained also from a complex simulation code OREBLA-REX. Fast oscillations of the emission current in OREB regimes are correctly treated by determining the diode voltage self-consistently. The feedback effects of various reflexing beam phenomena and role of ions changing the impedance of high-voltage diode are included.

REFERENCES

/1/ A.V.Arzhannikov et al.:Pisma Zh.Exp.Teor.Fiz., 27 (1978),173
/2/ C.B.Wharton et al.:Phys.Rev.Lett., 40 (1978),451
/3/ P.Šunka et al.:8th Europ.Conf. on Plasma Phys. and Contr.Nucl. Fus.Res., 1978, Prague
/4/ P.Šunka et al.:Plasma Phys.and Contr.Nucl.Fus.Res., 1976, Vol.II,IAEA, Vienna (1977)
/5/ A.V.Arzhannikov et al.:Pisma Zh.Exp.Teor.Fiz.24 (1976),76
/6/ P.Šunka et al.:Annual Progress Report, 1978, IPP-Czechoslovakia
/7/ D.C.Strew, R.B.Miller: IEEE Trans.Nucl.Sci., NS-24, No.3, (1977),1645
N.L.Olson:Fizika Plazmy, 3 (1977), 465 (in Russian)
/8/ K.Jungwirth:Proc.of the 10th Int.Symp. on Plasma Phys., 1979, IPP-Czechoslovakia
/9/ D.A.Phelps: IEEE Trans. on Plasma Sci., PS-6, No.1, (1978),76

COLLECTIVE INTERACTIONS OF MONOENERGETIC HIGH-ENERGY RELATIVISTIC ELECTRON BEAM WITH A DENSE PLASMA

A.K.Berezin, V.A.Kiselyov, Ya.B.Fainberg
Physico-Technical Institute, Acad. Sci. Ukr.SSR, Kharkov, USSR

1. It was theoretically shown [1-3] that during a collective electron beam-plasma interaction, HF - oscillations may develop in a plasma at a frequency W_p; the beam energy taken away to initiate these oscillations may be very high. Since high-current relativistic electron beams (REB) seem to be the most energetic, it would be reasonable to use them in order to obtain highly intensive HF-oscillations, provided that there is an efficient beam-plasma interaction.

This REB interaction efficiency, according to the theory, should increase with the plasma density growth. However, already first experiments with high-current REB indicated that the interaction efficiency falls down with the plasma density growth [4, 5]. This is attributed to the fact that in high-current REB the injection of electrons into plasma was performed under a high angle straggling, i.e. there was a high longitudinal-velocity straggling V_z in the beam. In this case a kinetic instability develops with the growth rate being

$$\delta \sim \omega_p \left(\frac{n_\beta}{n_p}\right) \frac{1}{\gamma} \frac{1}{\Delta\theta^2} \qquad (1)$$

where n_β is the beam density, n_p is the plasma density, $\Delta\theta$ is the angle straggling of beam electrons. This growth rate is small and it decreases with the plasma density increase ($\delta \sim n_p^{-1/2}$).

In the case of a monoenergetic beam with a low angle straggling $\Delta\theta$ we have a hydrodynamic instability with a growth rate.

$$\delta \sim \omega_p \left(\frac{n_\beta}{n_p}\right)^{1/3} \frac{1}{\gamma} \qquad (2)$$

which increases with the plasma density ($\delta \sim n_p^{1/6}$). More recent works [6] have demonstrated that with the lower angle straggling of electrons in high-current REBs the interaction effectiveness increases as the plasma density grows.

To study the efficiency of a collective REB-dense plasma interaction, experiments have been conducted with a monoenergetic beam having a relatively small current ($I_\beta \sim 1$A), but a high energy ($W \sim 2$ MeV and 20 MeV) and a low angle straggling ($\Delta\theta \sim 2.5 \cdot 10^{-3}$ rad)